Available online at www.sciencedirect.com
SCIENCE DIRECT®
Journal of Molecular Spectroscopy 233 (2005) 68–76
Journal of MOLECULAR SPECTROSCOPY
www.elsevier.com/locate/jms

# Water vapour line assignments in the 9250–26000 $cm^{-1}$ frequency range

Roman N. Tolchenov [a], Olga Naumenko [b], Nikolai F. Zobov [a,1], Sergei V. Shirin [a,1], Oleg L. Polyansky [c,1], Jonathan Tennyson [a,*], Michel Carleer [d], Pierre-François Coheur [d], Sophie Fally [d], Alain Jenouvrier [e], Ann Carine Vandaele [f]

[a] *Department of Physics and Astronomy, University College London, London WC1E 6BT, UK*
[b] *Russian Academy of Science, Institute of Atmospheric Optics, Tomsk 634055, Russia*
[c] *Sektion Spektren und Strukturdokumentation, University of Ulm, D-89069 Ulm, Germany*
[d] *Service de Chimie Quantique et Photophysique CPi160/09, Université Libre de Bruxelles, 50 Av. F.D. Roosevelt, B-1050 Brussels, Belgium*
[e] *Universit'e de Reims Champagne-Ardenne, Groupe de Spectrométrie Moléculaire et Atmosphérique, UFR Sciences, Moulin de la Housse B.P.1039, 51687 Reims Cedex 2, France*
[f] *Institut d'Aéronomie Spatiale de Belgique, 3 Av. Circulaire, B-1180 Brussels, Belgium*

Received 22 February 2005; in revised form 12 May 2005
Available online 20 July 2005

**Abstract**

Line parameters for water vapour in natural abundance have recently been determined for the 9250–13000 $cm^{-1}$ region [M.-F. Mérienne, A. Jenouvrier, C. Hermans, A.C. Vandaele, M. Carleer, C. Clerbaux, P.-F. Coheur, R. Colin, S. Fally, M. Bach, J. Quant. Spectrosc. Radiat. Transfer 82 (2003) 99] and the 13000–26000 $cm^{-1}$ region [P.-F. Coheur, S. Fally, M. Carleer, C. Clerbaux, R. Colin, A. Jenouvrier, M.-F. Mérienne, C. Hermans, A.C. Vandaele, J. Quant. Spectrosc. Radiat. Transfer 74 (2002) 493] using a high-resolution Fourier-transform spectrometer with a long-path absorption cell. These spectra are analysed using several techniques including variational line lists and assignments made. In total, over 15000 lines were assigned to transitions involving more than 150 exited vibrational states of $H_2{}^{16}O$. Twelve new vibrational band origins are determined and estimates for a further 16 are presented.


*Keywords:* Water vapour; Line assignments; Atmospheric radiation

## 1. Introduction

Understanding the rotation–vibration spectrum of water is central to constructing reliable models of the transmission of light through our atmosphere. Yet, particularly at the higher frequencies crucial for many atmospheric processes, this spectrum remains difficult to both characterise and interpret. Recently, some of us [1–3] have collaborated in a series of experiments to characterise the line parameters of water using a high-resolution Fourier-transform spectrometer with a long-path absorption cell. These studies, which considered the ranges 9250–13000 $cm^{-1}$ and 13000–26000 $cm^{-1}$, covered the entire visible region as well as extending into the near-infrared. The spectra were recorded by the Bruxelles-Reims groups and are collectively referred to as BR below.

A considerable number of previous laboratory measurements have been made of the near-infrared [4–8] and visible [7–10] wavelength spectra of water vapour in natural isotopic abundance. The complexity of weak

* Corresponding author. Fax: +44 20 7679 7145.
*E-mail address:* j.tennyson@ucl.ac.uk (J. Tennyson).
[1] Permanent address: Institute of Applied Physics, Russian Academy of Science, Uljanov Street 46, Nizhnii Novgorod 603950, Russia.

0022-2852/$ - see front matter © 2005 Elsevier Inc. All rights reserved.
doi:10.1016/j.jms.2005.05.015

rotation–vibration spectrum of water at these wavelengths has encouraged the development of assignment procedures based on variational nuclear motion calculations [11,12]. These have been widely applied to the spectrum of water vapour at near-infrared and visible wavelengths [13–19]. The result has been a considerable advance in our understanding of the spectroscopy of water in these regions, see [20] for example.

The new Fourier-transform spectra contained 7061 lines in the 9250–13 000 $cm^{-1}$ and 9353 lines in the 13 000–26 000 $cm^{-1}$ region, although, as discussed below, these lines contain a number of blends. Quantum number assignments for these transitions were based simply on the analysis of other spectra discussed above. However, since the new systematic spectra have already been included in the 2003 edition of the GEISA database [22] and is being prepared for inclusion in the 2004 edition of HITRAN [21], it is important that as complete and correct as possible set of assignments are made to these. In this work, we present a comprehensive analysis of the line assignments performed using a variety of methods but largely based on line lists generated using variational nuclear motion calculations. One advantage of analysing the present spectra is the broad spectral range studied which significantly reduces problems with edge effects when searching for combination differences. However, for convenience, much of the analysis was performed separately for the 9250–13 000, 13 000–16 000, and 16 000–26 000 $cm^{-1}$ regions, and these three regions will be considered separately below.

## 2. Experimental details

Detailed descriptions of the experimental setup and procedures have been given previously [2,15]. Briefly, the absorption spectra of water vapour were recorded using a high-resolution Fourier-transform Spectrometer (Bruker IFS120M) coupled to two White multiple-reflection cells of 5 and 50 m base path. The combination of two light sources (high-pressure Xenon arc and tungsten halogen) and two detectors (Si and GaP-diode) coupled to optical filters enabled us to cover the spectral region from 27 000 to 8000 $cm^{-1}$ in three overlapping ranges. Spectra with an absorption path of 600 m and a resolution of 0.06 $cm^{-1}$ (15 cm MOPD) were recorded in the near-UV and visible regions using the Xenon arc lamp. A resolution of 0.03 $cm^{-1}$ (MOPD of 30 cm) and absorption paths of 100 and 600 m were chosen to record the visible-NIR region using the tungsten halogen lamp. The temperature inside the cell was measured with three platinum wire thermometers which gave a 'room temperature' value of $292 \pm 3$ K. Table 1 summarises the spectra analysed here.

The co-addition of some 2000–4000 interferograms, leading to measurement times of 12–24 h, proved sufficient to get a signal-to-noise ratio (expressed as the maximum signal amplitude divided by twice the root-mean-square noise amplitude) better than 2500. The spectra were wavenumber calibrated using the $I_2$ visible spectrum. Pressure was measured with an MKS Baratron type manometer. Pure water vapour spectra were measured at various pressures from 6 to 18 hPa into the absorption cell. Additional spectra were recorded after adding $N_2$ or dry-air in the cell in four steps up to about 800 hPa, in order to measure the pressure effect on the lines shape and position. Data concerned with the line profiles have been presented previously [1–3] and are not re-analysed here.

Spectral line positions and other parameters were determined by fitting the lines with a Voigt profile using the procedure discussed previously [1–3]. The spectrum was treated in two separate regions: 9250–12 896 and 13 184–25 232 $cm^{-1}$. No transitions were observed above this frequency. The gap between 12 896 and 13 184 $cm^{-1}$ was found to contain no $H_2O$ lines although some transitions which could be assigned to the $O_2$ A-band and to HDO were observed.

The experimental line list contains 7061 lines in the 9250–12 896 $cm^{-1}$ region and 9353 between 13 184 and 25 232 $cm^{-1}$. In practise, particularly at lower frequencies, some of these lines are blends of more than one transition so the assigned line list presented here is somewhat longer. On the other hand, we have chosen to be more conservative than the original work of [1] in the higher-frequency region, and to remove from the final list a set of very weak lines, which could have been misidentified. Similarly, about 25 lines around 14 500 $cm^{-1}$ have been identified as probably due to transitions of $O_2$. The $O_2$ lines are listed in Table 2 and have been removed from our final line list.

## 3. Line assignments

Line assignments were performed in both London and Tomsk and iterated until an agreed set of parameters was obtained. The main means of assignment was

Table 1
Summary of experimental spectra analysed

| Region | Wavenumber ($cm^{-1}$) | Lamp | Detector | Resolution ($cm^{-1}$) | Path (m) |
|---|---|---|---|---|---|
| Near-UV–VIS | 27 000–17 000 | Xe | GaP | 0.06 | 600 |
| VIS | 23 000–10 000 | Xe | Si | 0.06 | 600 |
| VIS-NIR | 15 500–8000 | W | Si | 0.03 | 100 and 600 |

Table 2
Transitions, in $cm^{-1}$, due to molecular oxygen identified in the long path-length Fourier-transform spectrum of Coheur et al. [1]

| | | | | |
|---|---|---|---|---|
| 14468.8831 | 14468.9968 | 14478.2308 | 14480.1454 | 14486.9391 |
| 14495.1269 | 14502.8207 | 14504.7900 | 14509.9693 | 14518.7222 |
| 14522.7633 | 14531.0275 | 14535.7825 | 14535.9398 | 14544.0015 |
| 14545.9334 | 14549.2909 | 14550.1009 | 14552.2095 | 14554.3357 |
| 14555.3237 | 14555.7390 | 14556.5596 | 14557.8410 | 14557.9817 |

by comparison with line lists calculated using variational nuclear motion calculations. In the course of this work, more than three distinct line lists were used for this purpose. The first was the line list due to Partridge and Schwenke (PS) [12], which gives excellent frequency predictions for transitions below about 15000 $cm^{-1}$ but tends to overestimate the intensity of some transitions. The second was the line list recalculated by Tashkun (private communication) using the potential and parameters of PS, and the refitted dipole surface of Schwenke and Partridge [23]. This line list, denoted SP below, gives greatly improved intensities but remains unreliable for high frequencies. The third variational line list was a newly calculated line list based on the Fit B potential energy surface of Shirin et al. [24], the wavefunctions of Barber and Tennyson [25], and the dipole surface of Schwenke and Partridge. This line list, known as BT2, gives reliable frequencies for the whole range studied and, in particular at the higher frequencies, see Dupré et al. [26] for example.

The above-mentioned synthetic line lists were used as the input information for an expert system for automatic identification of rovibrational spectra [27] which was used in the assignment process. This system is based on the Rydberg–Ritz combination rule. It searches for combination differences in a large spectral interval, then chooses the best variant and, if approved by the researcher, inserts the corresponding assignments into the database for spectrum. Up to three assignments for the same absorption line are possible. At the final stage of the spectral assignment, when the database is almost completed, it is also possible to identify single lines not included among the ground-state combination differences, if the match between observed and calculated line position and intensity is believed to be reasonable.

In the course of the theoretical analysis, it became apparent that, particularly at the lower frequencies, many of the 'lines' identified in the original spectral studies were actually blends of two or more transitions. This finding is consistent with the somewhat anomalous linewidths and associated pressure dependence found for many of the lines. It was therefore decided to treat as blends all 'lines' which, in the theoretical calculations, were not dominated by a single transition.

Blended lines are identified in our final line list by the presence of more than one transition at a given frequency. The 296 K intensity of these transitions sums to that of the single 'line' given in the original BR line list but has been distributed between the lines using the theoretical intensity ratios. For this purpose, the SP and the BT2 line lists were used below and above 16000 $cm^{-1}$, respectively. Clearly, the use of a single frequency for all the lines in a blend is an approximation, but none of the theoretical line lists are accurate enough to be used to determine the (small) splittings between the lines. These can only be determined by careful fits to high-resolution experiments. Altogether considering blends increased the number of lines in the spectrum by about 11%.

When considering the assignment procedure below it is necessary to distinguish between assignment, which is the process of identifying the upper and lower states involved in a transition, and labelling, which is the process of associating each state with (approximate) quantum numbers. For the rotation–vibration states of $H_2{}^{16}O$ the only rigorous quantum numbers are the rotational angular momentum, $J$, the rotational parity $p$ and the interchange symmetry between the two H atoms, which determines whether the state is ortho or para. These quantum numbers are given rigorously by the various line lists used in this study. However, it is usual to label each state with vibrational quantum numbers, in either normal or local mode notation, and rotational quantum numbers $K_a$ and $K_c$.

In the course of analysing the present spectrum, we found a number of difficulties with the labelling used in previous studies. In particular, we found cases where the correct assignments had been obtained but the labels were inconsistent so, for example, two different states had been given the same quantum number labels. We also had some initial difficulty finding the correct labels for many of our new assignments. We therefore undertook a systematic (re-)labelling exercise based on analysis of the BT2 line list [25].

First, plots of the $J = 0$ vibrational wavefunctions were analysed to assign vibrational quantum numbers. Rotational levels associated with a vibrational state were identified using transition moments. To do this it was assumed that dipole transitions must be strongest between rovibrational levels belonging to the same vibrational state. Knowing labels for a $J$ level gives candidates for the levels in the same vibrational state with $J' = J + 1$. However, the maximum $J \leftrightarrow J + 1$ transition moment does not necessarily provide the correct label

for the $J+1$ level. As an approximate criterion it was assumed that the sum of the dipoles between levels within the same vibrational state must be the greatest. This procedure had to be iterated to get complete results.

It should be noted that one result of this procedure is the identification, discussed below, of transitions to many previous unobserved vibrational states. These new states are often characterised by only a few levels which are probably observed due to intensity stealing from a nearby bright state of the same symmetry.

The BR lines were published using previously known line assignments where available. In order to check and extend the assignments, we analysed the spectrum in three regions: 9250–13 000, 13 000–16 000, and 16 000–26 000 $cm^{-1}$. The split between the first and second region comes from the original experiments, and the break at 16 000 $cm^{-1}$ represents approximately the point where our new line list becomes more reliable than the SP one. Table 3 summarises the results of analysis in each of these regions. The region below 11 190 $cm^{-1}$ has been the subject of studies [6,18,19,28–30] which actually probe deeper than the BR results. The results for this region are therefore of less significance. Table 3 therefore also presents separate summaries of our results for this low-frequency region and the higher-frequency region for which the BR data now form the input for the HITRAN database [21].

In summarising the data in Table 3 we make a distinction between a reassignment, where a line is assigned to a completely distinct transition, and a re-labelling, where the upper level in a transition is of unchanged symmetry but has different (approximate) vibrational quantum numbers. It can be seen that we have made a large number of both new assignments and reassignments.

The BR spectra were recorded using water vapour with natural isotopic abundance. The spectrum therefore contains a number of lines not due to $H_2{}^{16}O$. These lines were identified by comparison with spectra of isotopically enriched spectra for $H_2{}^{17}O$ [31,35], $H_2{}^{18}O$ [32–35], and HDO [36–39].

Assignments are vital for determining the temperature-dependent absorption intensity of each line. They also yield information on the energy levels of the system. A complete set of the energy levels determined by analysing the BR spectra, which covers 150 vibrational states, is given in the electronic archive. Energy levels were determined from known ground-state levels [20] in two steps. First, using only unblended lines we calculated mean energies for those upper states which could be found with more than two transitions. Using the deviations from the mean values we estimated the error distribution with the line intensity and represented it as a linear function of intensity. In the second step, we calculated the final set of energy levels using this error distribution to weight the lines when evaluating the mean values. A comprehensive compilation of $H_2{}^{16}O$ energy levels was recently presented by Tennyson et al. [20] and we therefore concentrate only on differences from that compilation. Table 4 gives a numerical comparison of the newly determined energy levels. A complete listing of these new levels is given in the journal's electronic archive. We note that levels determined from blended lines are inherently less accurate so they are enumerated separately.

We made new assignments to the rotational ground levels of 12 excited vibrational bands. Also assignments to low-lying rotational levels for 16 other vibrational states allow us to obtain estimates for the vibrational band origins of these states guided by systematic differences between theory and experiment. This method of estimation has proved reliable in the past [16].

As implied above, a blended line will have a somewhat different line profile than a single line of the same

Table 3
Summary of our assignments of BR long path-length Fourier-transform water vapour spectrum by spectral region, in $cm^{-1}$, and isotopologue

| Region start ($cm^{-1}$): | 9250 | 13 184 | 16 000 | 9250 | 11 190 | 9250 |
|---|---|---|---|---|---|---|
| Region end ($cm^{-1}$): | 12 900 | 16 000 | 25 300 | 11 190 | 25 300 | 25 300 |
| Original lines | 7061 | 4755 | 4573 | 5534 | 10 855 | 16 389 |
| Extra blended lines | 985 | 409 | 412 | 851 | 953 | 1804 |
| Total lines | 8046 | 5162 | 4985 | 6385 | 11 808 | 18 193 |
| Observed lines assigned | 6573 | 4158 | 4279 | 5223 | 9787 | 15 010 |
| New assignments | 2193 | 558 | 1325 | 1732 | 2344 | 4076 |
| Reassignments | 916 | 130 | 137 | 832 | 351 | 1183 |
| Relabelled | 111 | 263 | 579 | 96 | 857 | 953 |
| De-assigned | 60 | 41 | 16 | 43 | 74 | 117 |

| Isotopologue | Total lines | Assigned |
|---|---|---|
| $H_2{}^{16}O$ | 16 990 | 15 621 |
| $H_2{}^{18}O$ | 736 | 734 |
| $H_2{}^{17}O$ | 255 | 246 |
| HDO | 212 | 212 |

Table 4
Summary of newly determined energy levels

| $v_1v_2v_3$ | $mn^{\pm}v_2$ | $\omega_0$ (cm$^{-1}$) | Levels | | |
|---|---|---|---|---|---|
| | | | Ref. [20] | New[a] | New[b] |
| 050 | 00 5 | 7542.44 | 105 | 2 | 4 |
| 130 | $10^{+}3$ | 8273.98 | 55 | 3 | 4 |
| 031 | $10^{-}3$ | 8373.85 | 229 | 5 | 7 |
| 210 | $20^{+}1$ | 8761.58 | 58 | 36 | 39 |
| 111 | $20^{-}1$ | 8807.00 | 209 | 16 | 23 |
| 012 | 11 1 | 9000.14 | 148 | 25 | 30 |
| 060 | 00 6 | 8870.6[c] | 37 | 11 | 13 |
| 140 | $10^{+}4$ | 9724.2 | 0 | 99 | 105 |
| 041 | $10^{-}4$ | 9833.59 | 144 | 33 | 42 |
| 220 | $20^{+}2$ | 10284.37 | 33 | 87 | 91 |
| 121 | $20^{-}2$ | 10328.73 | 86 | 56 | 63 |
| 022 | 11 2 | 10521.76[c] | 47 | 79 | 91 |
| 300 | $30^{+}0$ | 10599.69 | 83 | 54 | 60 |
| 201 | $30^{+}0$ | 10613.35 | 120 | 48 | 59 |
| 102 | $21^{+}0$ | 10868.88 | 73 | 49 | 55 |
| 003 | $21^{-}0$ | 11032.41 | 95 | 44 | 55 |
| 070 | 00 7 | 10086.0[c] | 3 | 25 | 28 |
| 051 | $10^{-}5$ | 11242.8 | 64 | 4 | 6 |
| 230 | $20^{+}3$ | 11767.39 | 37 | 8 | 11 |
| 131 | $20^{-}3$ | 11813.21 | 85 | 8 | 13 |
| 032 | 11 3 | 12007.78 | 42 | 9 | 15 |
| 310 | $30^{+}1$ | 12139.32 | 73 | 9 | 13 |
| 211 | $30^{-}1$ | 12151.25 | 122 | 1 | 4 |
| 112 | $21^{+}1$ | 12407.66 | 72 | 5 | 10 |
| 013 | $21^{-}1$ | 12565.01 | 88 | 3 | 6 |
| 160 | $10^{+}6$ | 12380.4[c] | 3 | 3 | 3 |
| 061 | $10^{-}6$ | 12586. | 26 | 3 | 5 |
| 240 | $20^{+}4$ | 13204.8[c] | 44 | 25 | 28 |
| 141 | $20^{-}4$ | 13256.2 | 49 | 8 | 12 |
| 042 | 11 4 | 13453.6 | 39 | 4 | 4 |
| 320 | $30^{+}2$ | 13640.7 | 77 | 10 | 15 |
| 221 | $30^{-}2$ | 13652.67 | 96 | 18 | 21 |
| 122 | $21^{+}2$ | 13910.90 | 66 | 14 | 18 |
| 023 | $21^{-}2$ | 14066.19 | 83 | 13 | 16 |
| 400 | $40^{+}0$ | 13828.28 | 100 | 10 | 11 |
| 301 | $40^{-}0$ | 13830.94 | 121 | 16 | 19 |
| 202 | $31^{+}0$ | 14221.16 | 102 | 9 | 11 |
| 103 | $31^{-}0$ | 14318.81 | 114 | 6 | 8 |
| 180 | $10^{+}8$ | | 0 | 5 | 6 |
| 004 | 22 0 | 14537.50 | 72 | 5 | 8 |
| 170 | $10^{+}7$ | 13660.6[c] | 6 | 3 | 4 |
| 071 | $10^{-}7$ | 13835.37 | 12 | 5 | 6 |
| 250 | $20^{+}5$ | | 1 | 9 | 12 |
| 151 | $20^{-}5$ | 14647.98[c] | 23 | 10 | 13 |
| 052 | 11 5 | | 1 | 6 | 6 |
| 330 | $30^{+}3$ | 15108.24 | 30 | 24 | 31 |
| 231 | $30^{-}3$ | 15119.03 | 72 | 8 | 12 |
| 132 | $21^{+}3$ | 15377.7 | 19 | 14 | 19 |
| 033 | $21^{-}3$ | 15534.71 | 64 | 6 | 8 |
| 410 | $40^{+}1$ | 15344.50 | 74 | 11 | 13 |
| 311 | $40^{-}1$ | 15347.96 | 93 | 8 | 9 |
| 212 | $31^{+}1$ | 15742.80 | 58 | 13 | 14 |
| 113 | $31^{-}1$ | 15832.77 | 85 | 10 | 12 |
| 260 | $20^{+}6$ | | 0 | 5 | 6 |
| 161 | $20^{-}6$ | | 0 | 7 | 7 |
| 014 | 22 1 | | 0 | 6 | 6 |
| 062 | 11 6 | | 0 | 8 | 8 |
| 340 | $30^{+}4$ | 16534.3 | 30 | 18 | 20 |
| 241 | $30^{-}4$ | 16546.32[c] | 35 | 20 | 20 |
| 142 | $21^{+}4$ | 16795.9[c] | 40 | 40 | 46 |
| 420 | $40^{+}2$ | 16823.32[c] | 51 | 20 | 21 |
| 321 | $40^{-}2$ | 16821.63 | 62 | 23 | 26 |
| 500 | $50^{+}0$ | 16898.4[c] | 81 | 10 | 12 |
| 401 | $50^{-}0$ | 16898.84 | 87 | 5 | 6 |
| 043 | $21^{-}4$ | 16967.6[c] | 18 | 11 | 11 |
| 270 | $20^{+}7$ | | 0 | 6 | 6 |
| 222 | $31^{+}2$ | 17227.38[c] | 40 | 11 | 15 |
| 123 | $31^{-}2$ | 17312.54 | 45 | 23 | 28 |
| 302 | $41^{+}0$ | 17458.35 | 63 | 11 | 12 |
| 203 | $41^{-}0$ | 17495.53 | 79 | 10 | 13 |
| 024 | 22 2 | | 0 | 5 | 6 |
| 104 | $22^{+}0$ | 17748.11[c] | 46 | 3 | 4 |
| 350 | $30^{+}5$ | | 0 | 9 | 9 |
| 251 | $30^{-}5$ | | 0 | 7 | 8 |
| 152 | $21^{+}5$ | | 0 | 12 | 12 |
| 331 | $40^{-}3$ | 18265.82 | 50 | 12 | 12 |
| 430 | $40^{+}3$ | 18267.1[c] | 4 | 45 | 8 |
| 053 | $21^{-}5$ | | 11 | 10 | 10 |
| 510 | $50^{+}1$ | 18392.97 | 34 | 25 | 25 |
| 411 | $50^{-}1$ | 18393.31 | 50 | 9 | 10 |
| 133 | $31^{-}3$ | 18758.63[c] | 23 | 18 | 21 |
| 312 | $41^{+}1$ | 0 | 10 | 10 | |
| 034 | 22 2 | | 8 | 4 | 4 |
| 213 | $41^{-}1$ | 18989.96 | 46 | 7 | 7 |
| 360 | $30^{+}6$ | | 0 | 7 | 7 |
| 261 | $30^{-}6$ | | 0 | 7 | 7 |
| 440 | $40^{+}4$ | 19677.8 | 0 | 31 | 34 |
| 341 | $40^{-}4$ | 19679.19[c] | 31 | 11 | 11 |
| 063 | $21^{-}6$ | | 3 | 5 | 6 |
| 600 | $60^{+}0$ | 19781.32[c] | 35 | 34 | 37 |
| 501 | $60^{-}0$ | 19781.10 | 53 | 20 | 20 |
| 520 | $50^{+}2$ | 19864.7[c] | 11 | 13 | 15 |
| 421 | $50^{-}2$ | 19865.28[c] | 15 | 4 | 5 |
| 044 | 22 4 | | 0 | 11 | 14 |
| 322 | $41^{+}2$ | | 0 | 9 | 9 |
| 223 | $41^{-}2$ | 20442.78[c] | 13 | 17 | 18 |
| 271 | $30^{-}7$ | | 0 | 4 | 5 |
| 402 | $51^{+}0$ | 20533.4[c] | 25 | 13 | 13 |
| 303 | $51^{-}0$ | 20543.14 | 32 | 9 | 9 |
| 105 | $42^{-}0$ | | 0 | 3 | 3 |
| 450 | $40^{+}5$ | | 0 | 10 | 11 |
| 351 | $40^{-}5$ | | 0 | 9 | 10 |
| 530 | $50^{+}3$ | | 0 | 15 | 16 |
| 431 | $50^{-}3$ | 21314.45[c] | 11 | 10 | 10 |
| 610 | $60^{+}1$ | 21221.5[c] | 9 | 32 | 34 |
| 511 | $60^{-}1$ | 21221.83 | 22 | 18 | 19 |
| 313 | $51^{-}1$ | 22015.4[c] | 0 | 8 | 8 |
| 460 | $40^{+}6$ | | 0 | 6 | 7 |
| 361 | $40^{-}6$ | | 0 | 5 | 5 |
| 115 | $42^{-}1$ | 22508.3[c] | 5 | 25 | 26 |
| 700 | $70^{+}0$ | 22529.29 | 42 | 20 | 22 |
| 601 | $70^{-}0$ | 22529.44 | 37 | 13 | 13 |
| 422 | $51^{+}2$ | | 0 | 4 | 4 |
| 403 | $61^{-}0$ | | 0 | 7 | 7 |
| 125 | $42^{-}2$ | | 0 | 9 | 9 |
| 710 | $70^{+}1$ | | 0 | 7 | 7 |
| 611 | $70^{-}1$ | 23947.1[c] | 9 | 1 | 2 |
| 800 | $80^{+}0$ | 25120.3[c] | 20 | 9 | 10 |
| 701 | $80^{-}0$ | 25120.28 | 24 | 5 | 6 |
| Total | | | 12258[d] | 1870[d] | 2140[d] |

Given are vibrational band origin, $\omega_0$, number of rotational term values determined, and numbers of new levels. Band origins given to less than 2 decimal places are estimates.

[a] Only strongest components of the blends have been used to calculate energy levels.

[b] All blend components have been used to calculate energy levels.

[c] Newly determined experimental values and estimates.

[d] Values including vibrational states not tabulated.

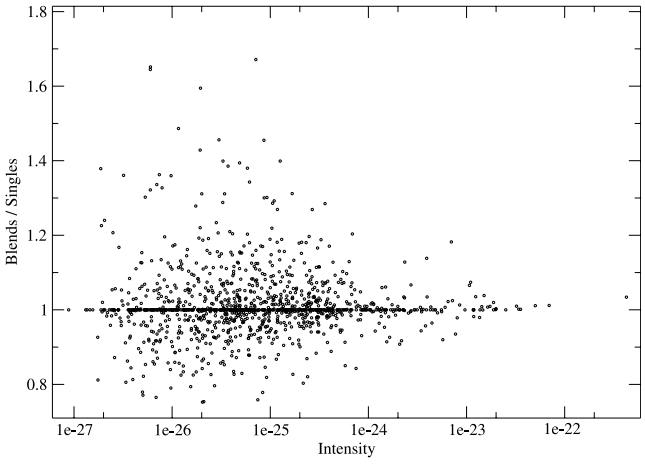


Fig. 1. Temperature dependence of the line intensity of transitions identified as blended when treated as blended compared to assigning all the line intensities to a single dominant transition. Intensities are calculated at temperature 316 °C and given in cm molecules$^{-1}$.

intensity. Furthermore, the intensity of a blended line will also display a temperature dependence which differs from that of the strongest line in the blend. To illustrate the effect of identifying the blended lines, Fig. 1 compares the predicted intensity of each of these lines for a temperature change of 20 °C. This sort of temperature change is typical of that found in an atmospheric column. It can be seen from the figure that for a number of lines the identification of the blend leads to significantly altered behaviour.

The splitting of the intensity of the blended lines according to the theoretical predictions of course relies heavily on the assumption that the calculated line intensities are accurate. Fig. 2 compares the line intensities

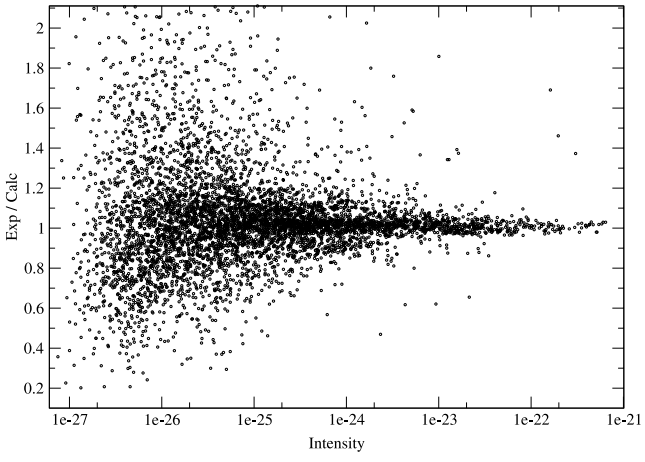


Fig. 2. Comparison of experimental line intensities with those calculated using the BT2 line list. Intensities, in cm molecules$^{-1}$, are for unblended transitions in the frequency range 9250–25 300 cm$^{-1}$ and are shown as function of the observed line intensity.

calculated with the BT2 line list [25] in the frequency range 9250–25 300 cm$^{-1}$ for transitions, which our analysis deemed unblended. It should be noted that our experience is that the transition intensities do not change significantly between calculations using the same dipole surface but different potential energy surfaces [40].

Fig. 2 shows very good agreement between the calculated and observed linestrengths for the strong transitions. For transitions intensities greater than $10^{-23}$ cm molecules$^{-1}$, the agreement is a few percent for all but three outliers. Not surprisingly, the disagreements get larger as the lines become less intense. As the uncertainties in both theory and experiment increase as the transition intensity drops, it is unclear which is the major cause of this increased disagreement.

## 4. Discussion and conclusion

The Fourier-transform spectra of water vapour of [1–3] provide a uniform treatment of absorption by natural isotopic abundance water vapour throughout the visible region of the spectrum. The latest release of HITRAN [21] uses these data for the entire visible region, a key region for atmospheric physics. Our analysis has significantly increased the number of assigned transitions in the spectrum and identified over 1800 lines which are actually blends of more than one transition. These blends explain some of the highly anomalous linewidths which were reported in the original study and largely ascribed to pressure broadening. 1205 lines due to the minor isotopologues of water have also been identified and 25 lines arising from absorption by molecular oxygen have been removed from the line list. This re-analysed line list, a complete copy of which has been placed in the electronic journal archive, has been submitted for inclusion in an updated version of HITRAN.

Among newly assigned transitions are those associated with excited bending states such as (060), (061), (160), (070), (170), and (071). The energy levels of such states give insight into the intramolecular dynamics of water for high excitation of the bending vibration which probes the potential close to linear geometries and which is accompanied by the abnormal centrifugal distortion effects [41]. Direct transitions to these high bending states are weak. However, the transitions assigned here are observable due to intensity borrowing from nearby strong lines. From the perspective of effective Hamiltonian theory, this intensity borrowing occurs via high-order resonance interactions. As a result the line list contains transitions identified with vibrational states with $v_2 > 7$. Although the energies of the corresponding rovibrational levels can be found in the electronic archive these states are not presented in Table 4. Labelling of highly excited bending states remains difficult. The

labelling procedure described above works well for states with low and medium $v_2$ but begins to fail for $v_2 > 7$. This may well be because at these high levels of excitation the strong coupling between vibrational states makes such labels rather arbitrary [42].

Spectral analysis shows that the most intense transitions to highly excited bending states very often involve, in contrast to nearby stretching states, upper levels with high values of $K_a$. This point is illustrated in Fig. 3 where the experimental and calculated intensity of the strongest transition to the upper level with a given value of $K_a$ is presented as a function of the generalised quantum number $N = J + K_a - K_c + 1$ for the $J = 9$ multiplet of the (201) stretching and the (060) bending state, respectively. It is clear from Fig. 3 that the intensity of the strongest transition to the (201) upper level belonging to the $J = 9$ multiplet smoothly decreases with increasing $K_a$. Conversely for the (060) state, there is a series of strong transitions (all observed in the spectrum) to the $K_a = 6$, 7, 8, and 9 upper levels. These transitions

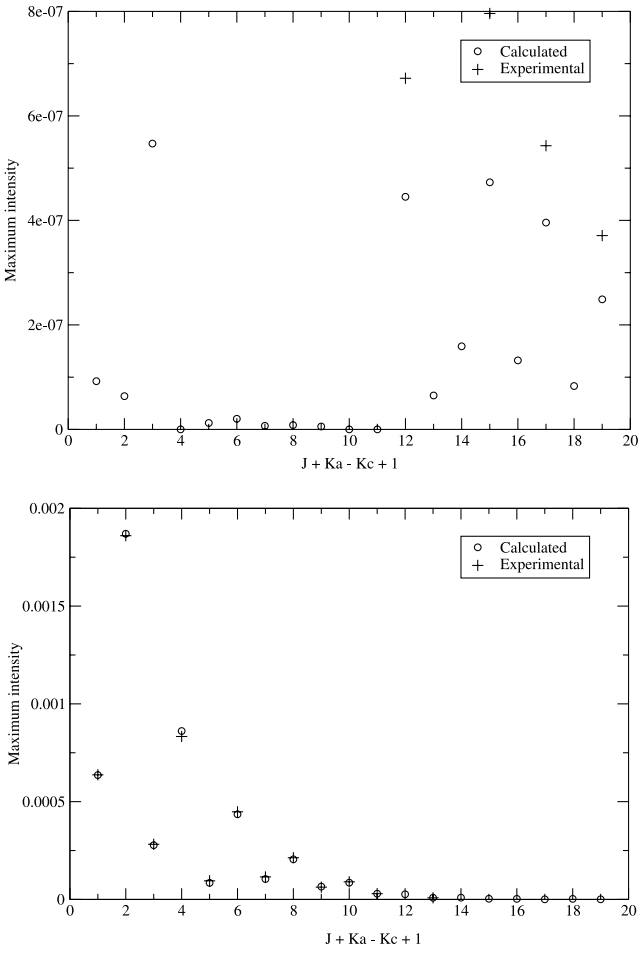


Fig. 3. Strongest transitions for $J = 9$ levels of (201) (upper panel) and (060) (lower panel) illustrating the different dependence on $K_a$. Intensities are given in $cm^{-2}$ $atm^{-1}$. Note the very different intensity scales.

borrow intensity from lines to levels associated with the neighbouring (300), (201), and (022) vibrational states. These may be separated from the interacting level of (060) level by up to 50 $cm^{-1}$. Furthermore, there is a relatively strong predicted transition to the $9_{18}$ level of (060) (not observed in the spectrum as it lies under an even stronger transition) which is caused by a clear resonance with the (111) state, the energy levels lying at 10 143 and 10 136 $cm^{-1}$, respectively. The cause of such relatively strong transitions to the high $K_a$ energy levels of the highly excited bending states is difficult to identify with confidence, since there are no energy levels of other states involving strong transitions in the vicinity of the considered bending levels. Intensity stealing from distant levels should only occur if the anharmonic resonance interaction increases strongly with both the bending $v_2$ and rotational $K_a$ quantum numbers.

The aim of this and related studies was to provide as complete and accurate database of water spectral parameters as can be achieved. It is therefore worth considering how the present line list can be improved. First, although the BR spectra were of high enough quality to detect many transitions due to the minor isotopologues of water, recording these spectra reliably using natural abundance water vapour is difficult. Spectra of $H_2{}^{17}O$ and $H_2{}^{18}O$ were recorded using isotopically enhanced samples more than two decades ago at Kitt Peak by Chevillard and co-workers [31,32]. These spectra are only now being properly analysed [33–35] but should provide good parameters for these molecules. New HDO spectra covering the near-infrared and visible spectral regions have been recorded by the Bruxelles-Reims group, using the same Fourier-transform technique and conditions as described in this study. A line list of HDO experimental line parameters in the 11 500–23 000 $cm^{-1}$ region will appear in a forthcoming paper [43]. This should provide excellent parameters for HDO which are entirely missing from HITRAN for this region.

We note that 18 of our newly determined $H_2{}^{16}O$ experimental energy levels were also recently observed [44] using cavity ring down spectroscopy (CRDS) in the 13 310–13 377 $cm^{-1}$ spectral region. The very high sensitivity provided by the CRDS technique allowed three times the number of the lines to be observed compared to this study within this limited spectral region. This CRDS study of water vapour and a similar one performed in the mid-infrared [45] have confirmed what was already suspected from theoretical analysis [46], as one looks deeper into the spectrum of water vapour more and more lines appear. There are a number of studies available [6,8,17–19,47] which probe deeper at the lower frequency end of the spectral range considered here. With the exception of the study by Brown et al. [6], these studies are most useful for characterising the position and strength of the weak lines. The studies are thus

largely complementary to the present work and a better database can be obtained by merging data from various sources. At present, however, the data for these weak transitions are only partial and more work needs to be done to obtain a complete picture.

This study follows a number of earlier ones using variational line lists to assign water transitions in the near-infrared and visible. The present study is very comprehensive in that there are few unassigned lines. However, it is anticipated that new spectra which probe even more deeply, such as the CRDS studies mentioned in the previous paragraph, will require further theoretical work.

## Acknowledgments

We thank Robert J. Barber for providing his $H_2{}^{16}O$ wavefunctions. This work was supported by the UK Natural Environment Research Council, the Royal Society, the INTAS foundation, the Russian Fund for Fundamental Studies, the Programme National de Chimie Atmosphérique (France), the Belgian Federal Science Policy Office, the European Space Agency (Contracts EV/11/03C and ESA-PRODEX C90-115), the Fonds National de la Recherche Scientifique (FNRS, Belgium), the ''Actions de Recherche Concertés'' (Communauté française de Belgique), and the European Union. O.L.P. is grateful for financial support from Dr. B. Mez-Starck foundation.

## References

[1] P.-F. Coheur, S. Fally, M. Carleer, C. Clerbaux, R. Colin, A. Jenouvrier, M.-F. Mérienne, C. Hermans, A.C. Vandaele, J. Quant. Spectrosc. Radiat. Transfer 74 (2002) 493–510.
[2] M.-F. Mérienne, A. Jenouvrier, C. Hermans, A.C. Vandaele, M. Carleer, C. Clerbaux, P.-F. Coheur, R. Colin, S. Fally, M. Bach, J. Quant. Spectrosc. Radiat. Transfer 82 (2003) 99–117.
[3] S. Fally, P.-F. Coheur, M. Carleer, C. Clerbaux, R. Colin, A. Jenouvrier, M.-F. Mérienne, C. Hermans, A.C. Vandaele, J. Quant. Spectrosc. Radiat. Transfer 82 (2003) 119–131.
[4] J.-P. Chevillard, J.-Y. Mandin, J.-M. Flaud, C. Camy-Peyret, Can. J. Phys. 67 (1989) 1065–1084.
[5] R.A. Toth, J. Mol. Spectrosc. 166 (1994) 176–183.
[6] L.R. Brown, R.A. Toth, M. Dulick, J. Mol. Spectrosc. 212 (2002) 57–82.
[7] R. Schermaul, R.C.M. Learner, D.A. Newnham, R.G. Williams, J. Ballard, N.F. Zobov, D. Belmiloud, J. Tennyson, J. Mol. Spectrosc. 208 (2001) 32–42.
[8] R. Schermaul, J.W. Brault, A.A.D. Canas, R.C.M. Learner, O.L. Polyansky, N.F. Zobov, D. Belmiloud, J. Tennyson, J. Mol. Spectrosc. 211 (2002) 169–178.
[9] C. Camy-Peyret, J.M. Flaud, J.Y. Mandin, J.P. Chevillard, J. Brault, D.A. Ramsay, M. Vervloet, J. Chauville, J. Mol. Spectrosc. 113 (1985) 208–228.
[10] J.Y. Mandin, J.P. Chevillard, C. Camy-Peyret, J.M. Flaud, J. Mol. Spectrosc. 116 (1986) 167.
[11] O.L. Polyansky, N.F. Zobov, S. Viti, J. Tennyson, P.F. Bernath, L. Wallace, Science 277 (1997) 346–349.
[12] H. Partridge, D.W. Schwenke, J. Chem. Phys. 106 (1997) 4618.
[13] O.L. Polyansky, N.F. Zobov, S. Viti, J. Tennyson, J. Mol. Spectrosc. 189 (1998) 291–300.
[14] D.W. Schwenke, J. Mol. Spectrosc. 190 (1998) 397.
[15] M. Carleer, A. Jenouvrier, A.-C. Vandaele, P.F. Bernath, M.F. Mérienne, R. Colin, N.F. Zobov, O.L. Polyansky, J. Tennyson, V.A. Savin, J. Chem. Phys. 111 (1999) 2444–2450.
[16] N.F. Zobov, D. Belmiloud, O.L. Polyansky, J. Tennyson, S.V. Shirin, M. Carleer, A. Jenouvrier, A.-C. Vandaele, P.F. Bernath, M.F. Mérienne, R. Colin, J. Chem. Phys. 113 (2000) 1546–1552.
[17] R.N. Tolchenov, J. Tennyson, J.W. Brault, A.A.D. Canas, R. Schermaul, J. Mol. Spectrosc. 215 (2002) 269–274.
[18] O. Naumenko, A. Campargue, J. Mol. Spectrosc. 221 (2003) 221–226.
[19] R.N. Tolchenov, J. Tennyson, S.V. Shirin, N.F. Zobov, O.L. Polyansky, A.N. Maurellis, J. Mol. Spectrosc. 221 (2003) 99–105.
[20] J. Tennyson, N.F. Zobov, R. Williamson, O.L. Polyansky, P.F. Bernath, J. Phys. Chem. Ref. Data 30 (2001) 735–831.
[21] L. Rothman et al., J. Quant. Spectrosc. Radiat. Transfer (in press).
[22] N. Jacquinet-Husson et al., J. Quant. Spectrosc. Radiat. Transfer. 95 (2005) 429.
[23] D.W. Schwenke, H. Partridge, J. Chem. Phys. 113 (2000) 16.
[24] S.V. Shirin, O.L. Polyansky, N.F. Zobov, P. Barletta, J. Tennyson, J. Chem. Phys. 118 (2003) 2124–2129.
[25] R.J. Barber, J. Tennyson, G.J. Harris, R.N. Tolchenov, Mon. Not. R. astr. Soc. submitted.
[26] P. Dupré, T. Germain, R.N. Tolchenov, N.F. Zobov, J. Tennyson, J. Chem. Phys. (in press).
[27] A.D. Bykov, O.V. Naumenko, A.M. Pshenichnikov, L.N. Sinitsa, A.P. Shcherbakov, Opt. Spectrosc. 94 (2003) 528–537.
[28] J.M. Flaud, C. Camy-Peyret, A. Bykov, O. Naumenko, T. Petrova, A. Scherbakov, L. Sinitsa, J. Mol. Spectrosc. 185 (1997) 211–221.
[29] J.M. Flaud, C. Camy-Peyret, A. Bykov, O. Naumenko, T. Petrova, A. Scherbakov, L. Sinitsa, J. Mol. Spectrosc. 183 (1997) 300–309.
[30] R.N. Tolchenov, J. Tennyson, J. Mol. Spectrosc. 231 (2005) 35.
[31] C. Camy-Peyret, J.-M. Flaud, J.-Y. Mandin, A. Bykov, O. Naumenko, L. Sinitsa, B. Voronin, J. Quant. Spectrosc. Radiat. Transfer 61 (1999) 795–812.
[32] J.-P. Chevillard, J.-Y. Mandin, J.-M. Flaud, C. Camy-Peyret, Can. J. Phys. 65 (1987) 777–789.
[33] A. Bykov, O. Naumenko, T. Petrova, A. Scherbakov, L. Sinitsa, J.-Y. Mandin, C. Camy-Peyret, J.-M. Flaud, J. Mol. Spectrosc. 172 (1995) 243–253.
[34] M. Tanaka, J.W. Brault, J. Tennyson, J. Mol. Spectrosc. 216 (2002) 77–80.
[35] M. Tanaka, O. Naumenko, J.W. Brault, J. Tennyson, J. Mol. Spectrosc. (to be submitted).
[36] O. Naumenko, E. Bertseva, A. Campargue, J. Mol. Spectrosc. 197 (1999) 122–132.
[37] O. Naumenko, A. Campargue, J. Mol. Spectrosc. 199 (2000) 59–72.
[38] E. Bertseva, O. Naumenko, A. Campargue, J. Mol. Spectrosc. 221 (2003) 38–46.
[39] O. Naumenko, S.M. Hu, S.G. He, A. Campargue, Phys. Chem. Chem. Phys. 6 (2003) 910–918.
[40] A. Callegari, P. Theule, R.N. Tolchenov, N.F. Zobov, O.L. Polyansky, J. Tennyson, J.S. Muenter, T.R. Rizzo, Science 297 (2002) 993–995.
[41] A. Bykov, O. Naumenko, L. Sinitsa, B. Voronin, J.-M. Flaud, C. Camy-Peyret, R. Lanquetin, J. Mol. Spectrosc. 205 (2001) 1–8.
[42] J.P. Rose, M.E. Kellman, J. Chem. Phys. 105 (1994) 7348–7363.
[43] M. Bach, S. Fally, P.-F. Coheur, M. Carleer, A. Jenouvrier, A.C. Vandaele, J. Mol. Spectrosc. (2005) in press.

[44] S. Kassi, P. Macko, O. Naumenko, A. Campargue, J. Mol. Spectrosc. (to be published).
[45] P. Macko, D. Romanini, S.N. Mikhailenko, O.V. Naumenko, S. Kassi, A. Jenouvrier, V.G. Tyuterev, A. Campargue, J. Mol. Spectrosc. 227 (2004) 90–108.
[46] R.C.M. Learner, W. Zhong, J.D. Haigh, D. Belmiloud, J. Clarke, Geophys. Res. Lett. 26 (1999) 3609–3612.
[47] H. Naus, W. Ubachs, P.F. Levert, O.L. Polyansky, N.F. Zobov, J. Tennyson, J. Mol. Spectrosc. 205 (2001) 117–121.